Surface vibrations of Ag(100) and Cu(100): A molecular-dynamics study

Liqiu Yang and Talat S. Rahman
Department of Physics, Cardwell Hall, Kansas State University, Manhattan, Kansas 66506-2601

Murray S. Daw
Theoretical Division, 8341, Sandia National Laboratories, Livermore, California 94551-0969
(Received 8 July 1991)

We present molecular-dynamics studies of Ag(100) and Cu(100), using interatomic potentials obtained by the embedded-atom method. The low-temperature results for the surface phonon frequencies and polarizations at selected points in the two-dimensional Brillouin zone are in good agreement with experimental data and also with results of first-principles calculations on both systems. The mean-square vibrational amplitudes of the surface atoms are found to be isotropic and much larger than the reported values for the bulk. As a function of increasing temperature, the frequencies of the surface phonons are found to redshift and the peaks to broaden. The variation of the mean-square vibrational amplitude with temperature displays effects of enhanced surface anharmonicity.

I. INTRODUCTION

The dynamics of the surfaces of several metals have been the subject of considerable examination as a result of continued developments in experimental probes and also in theoretical techniques used to understand the data. Among the issues being discussed are the frequencies and polarizations of the surface phonons and resonances, the dispersion of these normal modes, the mean-square vibrational amplitudes of the surface atoms, and the dependencies of all the above quantities on the surface temperature. While investigation of the surface dynamics at low temperatures can provide information on the bonding between surface atoms within the framework of a harmonic potential, studies for a range of higher temperatures are necessary to extract the role of surface anharmonicity and thermal roughening.

For the narrow range of issues in surface dynamics mentioned above, a good deal of experimental and theoretical efforts have focused on the (100), (111), and (110) surfaces of Ni, Ag, Au, Cu, and Pt. Although there are many peculiarities to each of these systems, a few general tendencies have also been found. For example, comparison of lattice-dynamical calculations with experimental data shows that the force constants between atoms in the surface layers are different from those in the bulk.[1–12] These deviations from the bulk values show certain characteristics: the (100) surface displays a stiffening in the interlayer surface force constant,[1,2] the (111) surface requires a softening in the surface intralayer force constant,[6–9] and the (110) surface, which has the highest propensity to reconstruct, demands the introduction of surface stress.[10–12] Furthermore, low-energy electron diffraction (LEED) and He-atom scattering from the (110) and (100) surfaces of Ni (Refs. 13 and 14) and Cu (Refs. 15–17) point to large increases in the mean-square vibrational amplitude of surface atoms and to the appearances of enhanced surface anharmonicity at characteristic temperatures.[13–15] Such an increase in surface anharmonicity has also been predicted by temperature-dependent electron-energy-loss-spectroscopy (EELS) measurements on Cu(110).[18]

In this paper we will confine our attention to Cu(100) and Ag(100) on which surface phonons have been the subject of recent investigations.[3–5] Lattice-dynamical calculations[4] based on force constants obtained from first-principles calculations reveal two modes—a longitudinal mode L_1 at $\bar{M}$ and a mode S_2 with first-layer longitudinal and second-layer shear vertical displacements at $\bar{X}$—which were not reported in earlier calculations using either parametrized force constants[2,3] or those obtained from an embedded-atom type of potential.[19] Although it is not easy to resolve the frequencies of these particular modes from the EELS data,[2–4] their presence leads to very good agreement between the calculated, incident energy-dependent cross sections for electron scattering and the measured values.

Our aim in this paper is first to calculate the frequencies and polarizations of all surface modes and resonances at the high-symmetry points in the two-dimensional Brillouin zone, using the molecular-dynamics (MD) technique based on interaction potentials obtained from the embedded-atom method (EAM).[20] A comparison of the results so obtained with the experimental data, as well as with the values obtained from theories based on first-principles calculations, is essential in testing the reliability of the phenomenological potential. It will be seen that the embedded-atom potential yields the frequencies and the polarizations of the surface vibrational modes in remarkable agreement with the calculations based on force constants derived from the first-principles method.[4]

The second and perhaps the main objective of the work is to extend the investigations of surface phonons to higher temperatures. This involves a systematic study of line broadening and frequency redshift as anharmonic

effects become important with increasing temperature. The effect of temperature on the mean-square vibrational amplitudes of atoms will also be explored and attention will be paid to enhancement in the vibrational amplitude of atoms in the first and the second layers of the crystal surface as compared to those in the bulk. So far several experiments suggest an increase in surface anharmonicity vis-à-vis its bulk value[16,17] for Cu(100). The calculations to be presented here will attest to this prediction.

The rest of this paper is organized as follows. Section II contains a summary of the theoretical technique involving the MD simulations and the procedure for obtaining the potentials using the embedded-atom method, Sec. III summarizes the results of the MD simulations for Cu(100) and Ag(100) at room temperatures and their comparison with experimental data and lattice-dynamical calculations based on force constants from first-principles methods and from parametrized fit to the data, Sec. IV focuses on the temperature-dependent dynamics of Cu(100), and Sec. V presents the conclusions.

II. THEORETICAL TECHNIQUE

A good review of the molecular-dynamics technique can be found in Ref. 21. Briefly, Newton's equations of motion of atoms, interacting via a given potential, are solved by using a suitable algorithm and by applying periodic boundary conditions to remove edge effects. The time evolution profile of the system, the radial distribution function, the velocity autocorrelation function, and the dynamical structure factor can thus be evaluated.

In the MD simulations to be presented here, the six-value Gear predictor-corrector algorithm,[21] with a time step of 1×10^{-15} sec in employed. Since the interaction potential is short ranged (~6 Å) the neighbor listing method[21] is employed to make the computation more efficient. Temperature of the system is controlled via the introduction of fictitious forces on atoms.[21] When the instantaneous temperature of the system is higher than the desired value, a frictional force is applied to each atom in order to slow it down and thus lowering the temperature. On the other hand, the temperature can also be increased by changing the sign of the frictional forces, i.e., accelerate each atom artificially along the direction of its velocity vector.

The procedure of the simulation is as follows. For each temperature to be studied, a zero-pressure bulk simulation is performed with 256 atoms arranged in a cube. Periodic boundary conditions are employed and the minimum image convention is used to calculate the interaction potentials for the atoms in the central cube. The size of the cube is allowed to fluctuate, thus allowing the determination of the equilibrium volume for the system under zero pressure. The lattice constant is extracted from the average volume $\bar{V}$ of the system. For the fcc structure with four repeating unit cells in each of the three Cartesian directions, the lattice constant $a_0=\bar{V}^{1/3}/4$. Thermal expansion is hence an inherent part of this procedure.

The lattice constant determined from the bulk simulation is used as input for the surface simulations. Periodic boundary conditions and the minimum image convention are now invoked in the two directions parallel to the surface plane and no boundary conditions are used along the surface normal. The slab contains ten layers with a 10×10 square lattice in each layer, giving a total of 1000 atoms in the system. For each surface at each temperature, the perfect lattice positions of the truncated surface are used as initial configurations of the atoms. Initial velocities are drawn from Maxwell distribution at the particular temperature. A 10-ps constant-temperature equilibration run is made to ensure that the surface relaxation process has completed and that the system is equilibrated at the desired temperature. Afterwards, the system is left undisturbed in a 50-ps constant-energy simulation during which the positions and velocities of the atoms are stored for analyses of structural and dynamical properties of the system such as the mean-square vibrational amplitudes of atoms and the phonon spectral densities.

The mean-square displacement (MSD) from the equilibrium position (mean-square vibrational amplitude) of an atom in the jth layer is defined as

$$\langle u_j^2\rangle=\frac{1}{N_s}\sum_{i=1}^{N_s}\langle[\mathbf{r}_i(t)-\langle\mathbf{r}_i(t)\rangle]^2\rangle\ , \tag{1}$$

where N_s is the number of atoms per layer, $j=1$ is the surface layer, and $\langle\ \rangle$ represents an average over time t.

The surface phonon spectral densities can be calculated from the dynamic structure factor,[22] or in the one-phonon approximation, from the temporal Fourier transform of the layer-averaged displacement-displacement autocorrelation functions.[23] Since the reference positions for the atomic displacements are not well defined, we use velocities instead of displacements to analyze the vibrational frequencies.[24] The surface phonon spectral densities are then obtained from the temporal Fourier transform of the layer-averaged velocity-velocity autocorrelation functions according to

$$g_{\alpha\alpha}(\mathbf{Q}_\parallel,\omega)=\int e^{i\omega t}\left\langle\left[\sum_{j=1}^{N_s}e^{i\mathbf{Q}_\parallel\cdot\mathbf{R}_j^0}v_{j\alpha}(t+\tau)\right]\left[\sum_{j=1}^{N_s}e^{-i\mathbf{Q}_\parallel\cdot\mathbf{R}_j^0}v_{j\alpha}(\tau)\right]\right\rangle_\tau dt\ , \tag{2}$$

where $\mathbf{R}^0$ is the equilibrium position of an atom and $\langle\ \rangle_\tau$ represents an average over the starting times τ. One could use Eq. (2) directly to obtain the phonon spectral densities, but the correlation functions for the solid phase, especially at low temperatures, do not decay to zero very rapidly and thus the truncation error, after a Fourier transform, can cause negative peaks in the spectral density curve. For the results we will present later,

the phonon spectral densities are obtained according to

$$g_{\alpha\alpha}(\mathbf{Q}_{\parallel},\omega)=\left|\int e^{i\omega t}\left[\sum_{j=1}^{N_s} e^{i\mathbf{Q}_{\parallel}\cdot\mathbf{R}_j^0} v_{j\alpha}(t)\right]dt\right|^2 . \quad (3)$$

In the event that the simulation time approaches infinity, it can be proved rigorously that Eqs. (2) and (3) are equivalent.[22] The raw spectrum obtained according to Eq. (3) is smoothed by convoluting it with a Gaussian function, to eliminate the noise caused by an insufficient number of averages.[22]

In addition to the above dynamical quantities, structural information like interlayer relaxation can also be calculated directly from the difference between the average heights (the z coordinates) of the first and second layers:

$$d_{12}=\frac{1}{N_s}\left\langle\left[\sum_{i=1}^{N_s} z_i(t)-\sum_{i=N_s+1}^{2N_s} z_i(t)\right]\right\rangle_t . \quad (4)$$

Now let us turn to the central issue in a MD simulation, the interaction potentials. We choose the embedded-atom-method potential because of its many-body nature and the overall success in reproducing surface relaxations[25] and bulk[8] and surface phonon dispersion[8,19] for several metallic systems. The total potential energy of the homonuclear solid has the following form in the EAM:

$$E_{\rm tot}=\sum_i F\left[\sum_{j(\neq i)}\rho^a(r_{ij})\right]+\tfrac{1}{2}\sum_{i,j\neq i}\phi(r_{ij}) , \quad (5)$$

where the embedding function F is a functional of the electronic charge density with origins in the density-functional theory,[26] ρ^a is the angle-averaged radial electronic charge density function obtained from the Hartree-Fock calculations for free atoms,[27] ϕ is the pairwise repulsion between the cores of atoms, and r_{ij} is the separation between atoms i and j. It can be shown that the first term on the right-hand side of Eq. (5) represents a many-body type of interaction if F is a nonlinear function, but reduces to a pair interaction otherwise.[20] The forms of embedding function of several fcc metals are chosen to be cubic splines fitted to bulk experimental data such as the sublimation energy, equilibrium lattice constant, elastic constants, and vacancy-formation energies of the pure metals and the heats of solution of the binary alloys.[25] When applied to solid surfaces, the parameters for the potential are not changed, nor are additional adjustable parameters introduced. Therefore, the model is surface parameter free. References to the application of the EAM to a variety of problems in pure metals and alloys, including studies on phonon dispersion, thermal-expansion coefficient, liquid-metal structure, surface reconstruction, point defects, dislocation motion and fracture of pure metals, and segregation of alloys at interfaces, can be found elsewhere.[28]

The force acting on atom k is expressed as

$$\mathbf{f}_k=-\frac{dE_{\rm tot}}{d\mathbf{r}_k} \quad (6)$$

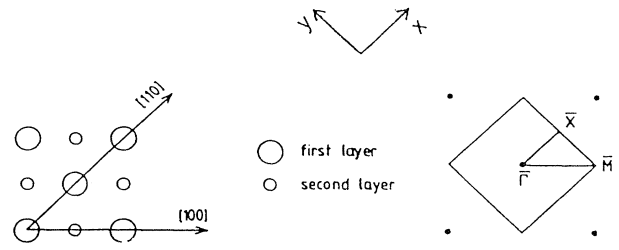

FIG. 1. The top view of the fcc(100) surface and the two-dimensional Brillouin zone.

and the pressure of the system is defined as

$$P=\frac{N}{V}k_B T-\left\langle\frac{dE_{\rm tot}}{dV}\right\rangle_{N,T} . \quad (7)$$

With Eqs. (5)–(7) and the input of the three functions F, ρ^a, and ϕ, one can now perform MD simulations with the EAM potentials.

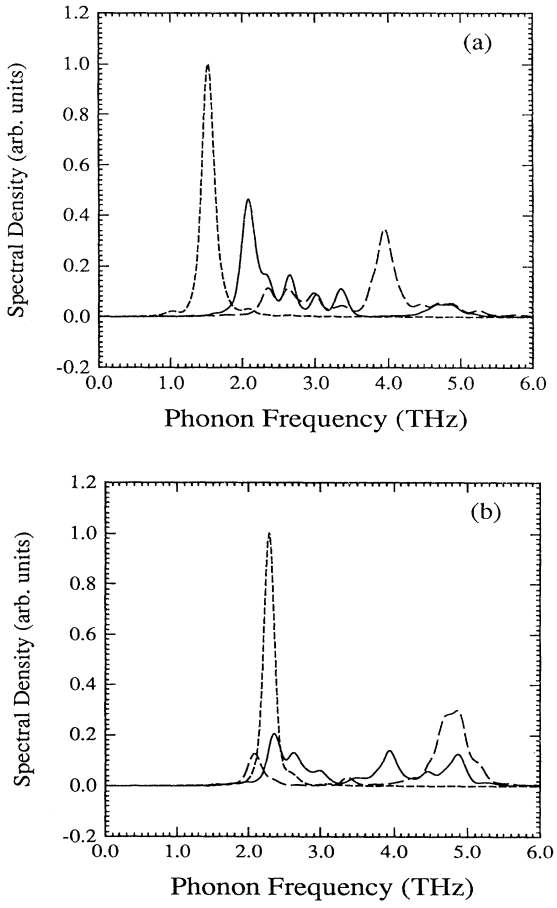

FIG. 2. Surface phonon spectral densities of AG (100) at 300 K at $\bar{X}$ for (a) the first-layer atoms and (b) the second-layer atoms. In this and all subsequent figures on surface phonon spectral densities, the solid, long-dashed, and short-dashed lines represent the shear vertical, longitudinal (even), and shear horizontal (odd) components, respectively.

III. SURFACE PHONONS OF Cu(100) AND Ag(100) AT ROOM TEMPERATURE

The geometry of the fcc(100) surface and the two-dimensional Brillouin zone are shown in Fig. 1. The phonon spectral densities for the displacements of the first- and second-layer atoms as obtained from the MD simulations discussed above, are presented in Figs. 2–5. The results for Ag(100) at the $\bar{X}$ point in the two-dimensional Brillouin zone in Fig. 2(a) show the shear horizontal mode (odd) S_1 at 1.55 THz, the shear vertical mode S_4 (the Rayleigh wave) at 2.1 THz, and the longitudinal mode S_6 at 3.95 THz. All three of these modes have their maximum amplitude in the first layer. The spectral densities in Fig. 2(b) for the displacements of the atoms in the second layer reveal another mode S_2 at 2.3 THz with shear vertical motion in the second layer coupled to longitudinal motion of atoms in the first layer. Other features in Fig. 2(b) include the second-layer shear horizontal mode at 2.3 THz, the S_4 mode at 2.1 THz with longitudinal polarization in the second layer, the S_6 mode at 3.95 THz with vertical motion of the second-layer atoms, and a resonance at 2.65 THz associated with a vertical displacement of atoms. Note that in each figure the maximum value of the spectral density has been put to unity and the area under each curve is the same. Thus S_2 resonance which lies inside the bulk band is stronger than what is apparent from the figure.

The spectral densities for Ag(100) at $\bar{M}$ presented in Fig. 3(a) display the S_1 (shear vertical) mode at 2.78 THz outside the bulk band and the degenerate modes L_1 (longitudinal) and L_1' (odd, shear horizontal) at 3.4 Hz. Similarly, the spectral densities for the atoms in the second layer in Fig. 3(b) exhibits the S_2 mode with vertical polarization at 3.4 THz and the L_1 and L_1' modes at 3.4 THz which continue to have the same polarizations as the atoms in the first layer.

The highlights of the spectral densities of Cu(100) are very similar to that of Ag(100). At $\bar{X}$, the modes in the first layer, shown in Fig. 4(a), are S_1 (shear horizontal) at 1.91 THz, the Rayleigh wave S_4 (shear vertical) at 2.91 THz, S_6 (longitudinal), a doublet at 5.77 and 5.95 THz, and S_2 (longitudinal first layer and shear-vertical second layer) at 3.77 THz. The frequencies and polarizations of the modes in the second layer are shown in Fig. 4(b).

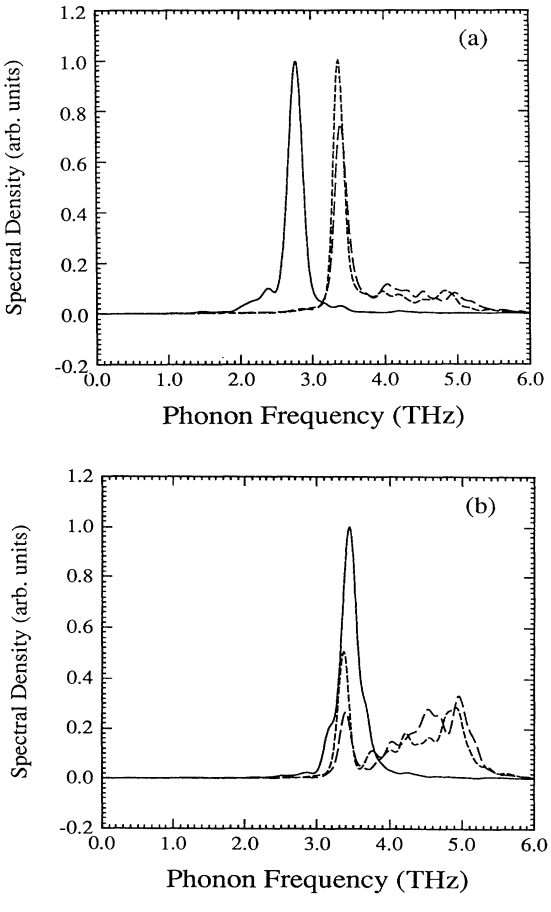

FIG. 3. Surface phonon spectral densities of Ag(100) at 300 K at $\bar{M}$ for (a) the first-layer atoms and (b) the second-layer atoms.

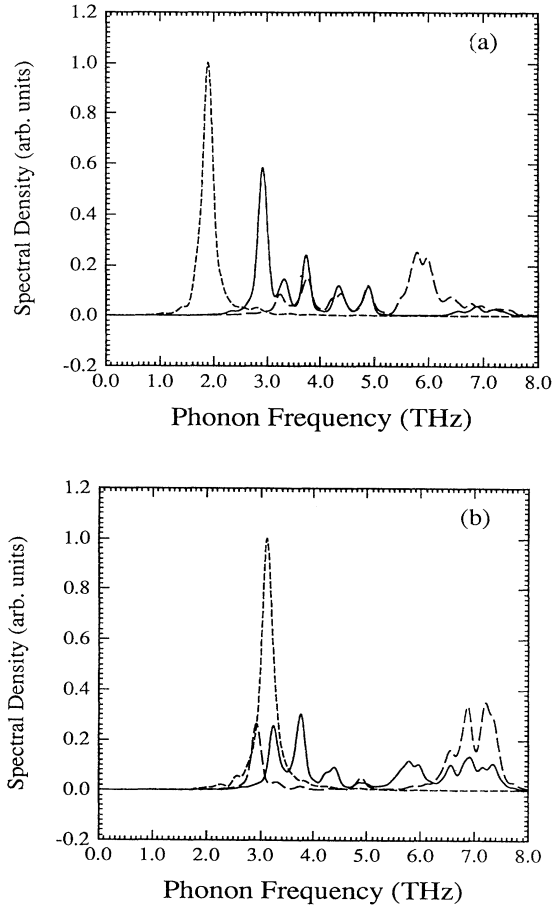

FIG. 4. Surface phonon spectral densities of Cu(100) at 300 K at $\bar{X}$ for (a) the first-layer atoms and (b) the second-layer atoms.

These two figures also indicate that for S_2 the first-layer atoms have vertical, as well as longitudinal, displacements. Note that in both Figs. 4(a) and 4(b) there is also a mode at 3.22 THz with polarization similar to that of S_2. Further detailed MD simulations with a larger number of layers will be more helpful in assigning the origin of the mode at 3.22 THz. Finally, the spectral densities for Cu(100) at $\bar{M}$ are presented in Figs. 5(a) and 5(b), displaying the S_1, L_1, and S_2 modes, similar to the case for Ag(100).

A comparison of the frequencies of the modes at $\bar{X}$ and $\bar{M}$ for Ag(100) and Cu(100) obtained by several theoretical techniques is summarized in Tables I and II. The results presented in Figs. 2–5 are tabulated under the method heading MD/EAM. We have also performed calculations using the lattice dynamical technique with parametrized surface force constants and the nearest neighbor (NN) interactions.[1,29] The results for Ag(100) obtained by choosing $k_{12}=1.2k$ and $k_{11}=0.8k$, where $k=20{,}200$ dyn/cm is the bulk force constants, are under LD/NN in Table I. Here k_{12} is the force constant between atoms in the surface layer and the layer below and k_{11} is the coupling between the atoms within the surface layer. Similar results for Cu(100) with $k_{12}=1.2k$ and $k=27{,}000$ dyn/cm are presented in Table II under method LD/NN. The frequencies obtained using lattice dynamics techniques with surface force constants from first-principles (FP) calculations,[4,5] the EAM (Ref. 19) and bulk parameters [4NN (Ref. 31) and 2NNα (Ref. 30)] are also contained in the tables. Here 4NN and 2NNα refer to the models with four nearest-neighbor central force interactions, and two nearest-neighbor interactions plus angle-bending interactions between nearest neighbors, respectively.

Chen *et al.*[4,5] have claimed that force constants from first-principles calculations yield new modes, L_1 at $\bar{M}$ and S_2 at $\bar{X}$, whose eigenvectors are crucial to the understanding of the energy dependence of the scattering cross-section of the modes observed in EELS (Refs. 4, 5, and 32) and the feature spread between 3.6 and 4.1 THz in He-scattering data[33] on Cu(100) near $\bar{X}$. It is true that the earlier studies on those two systems had not reported the L_1, or the S_2 mode, as the tables reflect. However, the molecular dynamics results presented here, as well as, the lattice dynamical calculations with parametrized force constants do reproduce both the L_1 and S_2 modes with frequencies in good agreement with the experimental data and the theoretical results in Refs. 4 and 5.

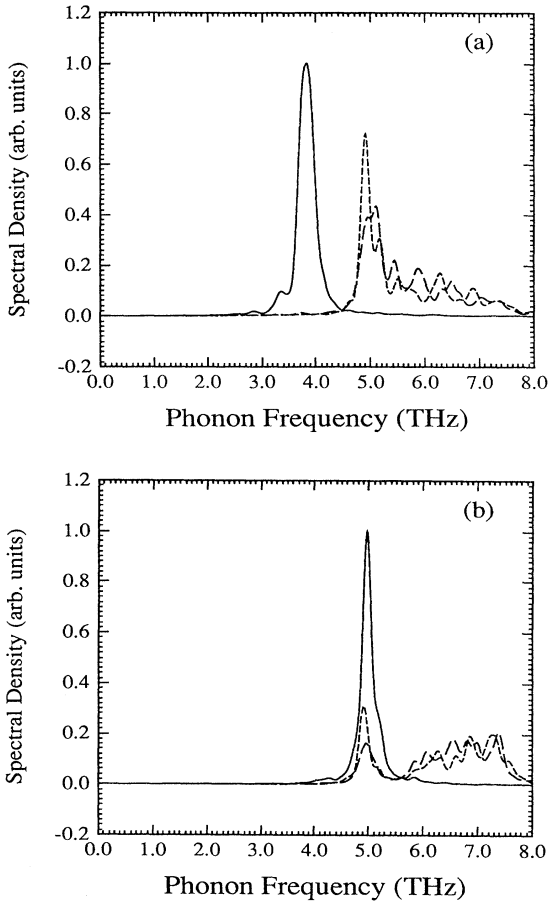

FIG. 5. Surface phonon spectral densities of Cu(100) at 300 K at $\bar{M}$ for (a) the first-layer atomms and (b) the second-layer atoms.

TABLE I. Comparison of surface phonon frequencies for Ag(100) (in units of THz).

	$\bar{M}$t			$\bar{X}$			
Method	$S_1(z)$	$L_1(x+y)$	$S_2(z_2)$	$S_1(y)$	$S_4(z)$	$S_2(z_2)$	$S_6(x)$
Expt.	2.4[a]			0.8[b]	2.1[a]		
MD/EAM	2.78	3.40	3.48	1.55	2.10	2.35	3.95
LD/NN	2.58	3.25	3.52	1.85	2.12	2.54	3.94
LD/FP[a]	2.5	3.3	3.2–3.4	1.4	2.1	2.2	4.1
LD/2NN[c]	1.82		3.35	0.86	2.09		4.08
LD/4NN[d]	2.1			1.4	1.8		4.2

[a] Reference 5.
[b] Reference 34.
[c] Reference 30.
[d] Reference 31.

TABLE II. Comparison of surface phonon frequencies for Cu(100) (in units of THz).

	$\bar{M}$			$\bar{X}$			
Method	$S_1(z)$	$L_1(x+y)$	$S_2(z_2)$	$S_1(y)$	$S_4(z)$	$S_2(z_2)$	$S_6(x)$
Expt.[a,b,c]	4.05		4.9		3.24	3.6–4.1	6.1
MD/EAM	3.88	5.10	4.99	1.91	2.91	3.77	5.77
LD/NN	3.95	5.15	5.32	2.79	3.20	4.08	6.14
LD/FP[a]	4.3	5.0	4.9	2.3	3.1	3.4	6.2
LD/EAM[d]	3.97			2.09	2.99		6.08
LD/2NNα[e]	3.66		5.18	2.59	3.11		6.11

[a] Reference 4.
[b] Reference 32.
[c] Reference 33.
[d] Reference 19.
[e] Reference 30.

IV. TEMPERATURE-DEPENDENT DYNAMICS OF Cu(100)

The MD simulations have been carried out for Cu(100) at 150, 300, and 600 K. The results for the phonon frequencies at 300 K have already been reported in Sec. III. In Figs. 6(a) and 6(b), the phonon spectral densities for the first layer atoms at $\bar{X}$ at surface temperatures of 150 and 600 K, respectively, are displayed. As expected, the features in Fig. 6(a), including the S_6 mode which appeared broad in Fig. 4(a), are sharp and they broaden out considerably in Fig. 6(b), as a result of anharmonicity in

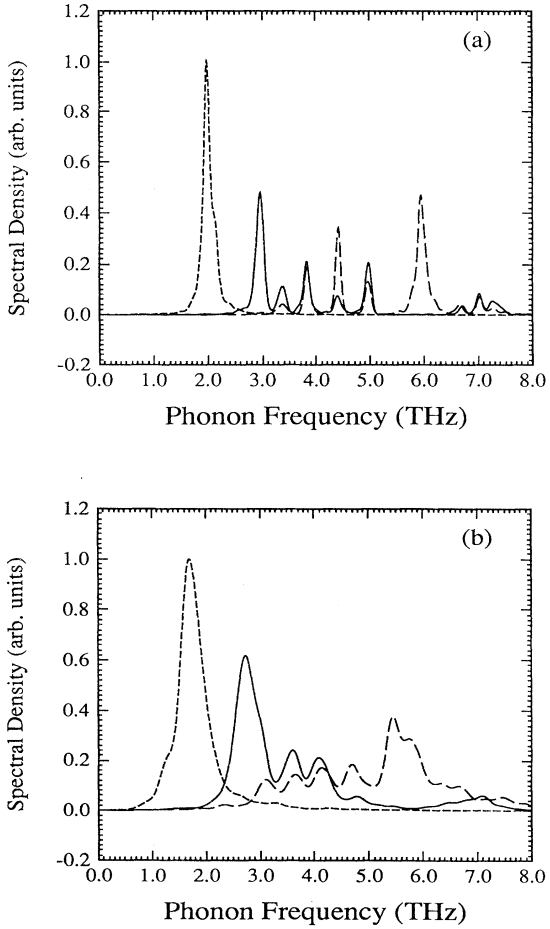

FIG. 6. Surface phonon spectral densities of Cu(100) at $\bar{X}$ for the first-layer atoms at (a) 150 K and (b) 600 K.

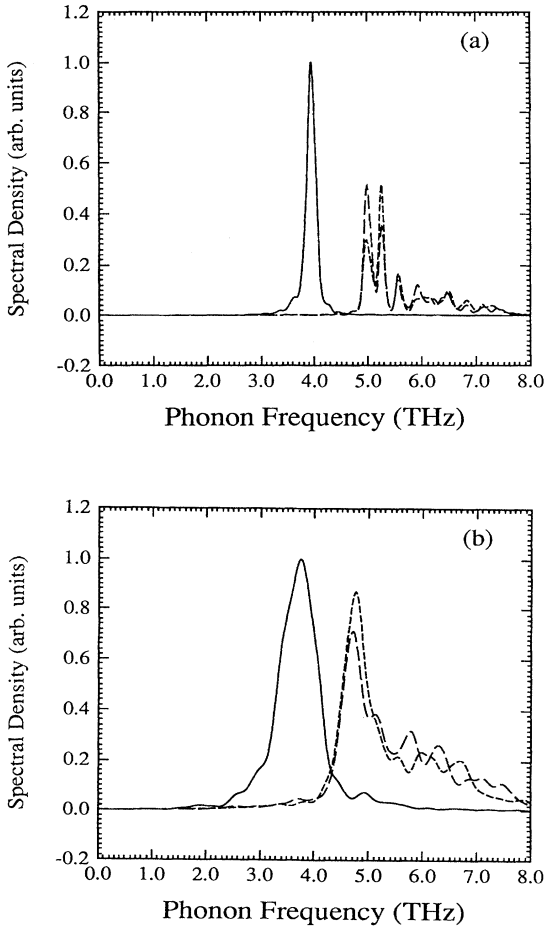

FIG. 7. Surface phonon spectral densities of Cu(100) at $\bar{M}$ for the first-layer atoms at (a) 150 K and (b) 600 K.

TABLE III. Phonons at $\bar{X}$ on (100) surfaces (phonon frequency ± half width at half maximum in units of THz). (Asterisks denote weak and broad peaks.)

Metal	Temp.	$S_1(y)$	$S_4(z)$	$S_z(z_2)$	$S_6(x)$
Ag	300 K	1.55±0.07	2.10±0.09	2.35*	3.95±0.17
Cu	150 K	2.02±0.06	3.00±0.07	3.81±0.04	6.00±0.08
	300 K	1.91±0.09	2.91±0.08	3.77±0.08	5.77±0.25
	600 K	1.78±0.22	2.72±0.26	3.68*	5.42±0.34

TABLE IV. Phonons at $\bar{M}$ on (100) surfaces (phonon frequency ± half width at half maximum in units of THz).

Metal	Temp.	$S_1(z)$	$L_1(x+y)$	$S_2(z_2)$
Ag	300 K	2.78±0.09	3.40±0.07	3.48±0.11
Cu	150 K	4.00±0.08	5.25±0.05	5.18±0.06
	300 K	3.88±0.15	5.10±0.18	4.99±0.07
	600 K	3.80±0.38	4.71±0.36	4.80±0.28

TABLE V. Interlayer relaxation on (100) surfaces with distances in units of Å.

Metal	Temp.	a_0	d_{bulk}	d_{12}	$d_{12}-d_{\text{bulk}}$	$(d_{12}-d_{\text{bulk}})/d_{\text{bulk}}$
Ag	300 K	4.114	2.057	2.021	−0.036	−1.750%
Cu	150 K	3.624	1.812	1.788	−0.024	−1.325%
	300 K	3.633	1.817	1.795	−0.022	−1.211%
	600 K	3.652	1.826	1.810	−0.016	−0.876%

TABLE VI. Mean-square vibrational amplitude on (100) surfaces and the one-dimensional bulk value in units of 10^{-2} Å^2.

Metal	Temp.	$\langle u^2_{1\perp}\rangle$	$\langle u^2_{1\parallel}\rangle$	$\langle u^2_{2\perp}\rangle$	$\langle u^2_{2\parallel}\rangle$	$\langle u^2_{\text{bulk}}\rangle$
Ag	300 K	1.52	1.38	1.13	0.96	0.8
Cu	150 K	0.61	0.59	0.44	0.42	0.3
	300 K	1.28	1.30	0.92	0.88	0.7
	600 K	2.80	3.06	1.94	2.03	1.4
	900 K	5.09	6.24	3.64	3.93	2.4

the interaction potential.

It is of interest to also look at the spectral density for Cu(100) at $\bar{M}$, particularly at 150 K shown in Fig. 7(a). There are two distinct modes with longitudinal polarization in the first layer at 4.95 and 5.25 THz. At higher temperatures, however, only one such feature survived [See Figs. 5(a) and 7(b)]. Most likely the lower frequency mode (~ 5 THz) arises from the large density of states at the edge of the bulk band while the higher frequency (5.25 THz at 150 K) is the L_1 resonance discussed earlier. As a function of increasing temperature the phonon spectral densities not only broaden but the peak positions also shift downward in frequency. These variations in the frequencies and the linewidth for Cu(100) are summarized in Tables III and IV. To date we are unaware of any experimental data on such temperature effects. For comparison, the values for Ag(100) at 300 K are also included in the tables.

Apart from reproducing the surface phonon frequencies and polarization remarkably well, the EAM potential is also able to yield interlayer surface relaxation.[25] The calculated values of the lattice constant a_0, the bulk interlayer separation d_{bulk}, and the separation between the first and the second layer d_{12}, at three temperatures, are illustrated in Table V. Our value of -1.2% contraction for the surface layer in Cu(100) at 300 K is more in agreement with the low-energy-electron-diffraction data[35] (-1.1%) than that concluded from the medium-energy ion scattering experiments.[36] We are not aware of similar data on Ag(100). The table also shows that the linear (vertical) expansion coefficient at the Cu(100) surface is approximately 2.79×10^{-5}/K and that in the bulk is about 1.65×10^{-5}/K, in agreement with previous EAM calculations[28] and experimental data[37] on bulk Cu.

Finally, the mean-square vibrational amplitudes of the first- and second-layer atoms are summarized in Table VI. For the (100) surface of both Ag and Cu, the mean-square vibrational amplitudes of the surface atoms are almost isotropic except at 900 K for Cu, bearing in mind a statistical error of $\pm0.05\times10^{-2}$ Å^2 in our calculated values. However, some finer trends towards anisotropic behavior can be seen from the numbers presented in the table. For Ag(100) at 300 K the out-of-plane mean-square vibrational amplitude is larger than the in-plane one by about $\sim 10\%$. For Cu(100) we find almost no anisotropy until 600 K, but a trend for the in-plane mean-square vibrational amplitude to dominate as the temperature increases. This is understandable since the surface is eventually going to disorder with in-plane diffusion of adatoms. Experimentally, isotropic behavior has been reported on Ag(100) in earlier work using back-diffracted low-energy electrons,[38] and on Ag(111),[39] and more recently for the Ni(100) (Ref. 14) surface atoms. The conclusion from recent medium-energy ion scattering experiments,[36] however, suggests that on Cu(100) the out-of-plane vibrational amplitudes are smaller than the in-plane one by 30%. Earlier lattice-dynamical calculations based on bulk force constants and for harmonic systems,[40] and also calculations treating anharmonic terms through perturbative schemes,[41] had found the out-of-plane vibrational amplitudes at metal surfaces to be larger than the in-plane ones by about 50%. We await further work to clarify the situation. Finally, it should be pointed out that our values for the mean-square vibrational amplitudes in bulk Cu are in reasonable agreement with those calculated by Ma, deWette, and Aldredge[41] at 150 K, but not at higher temperatures. The perturbative results are consistently lower than values reported in Table VI.

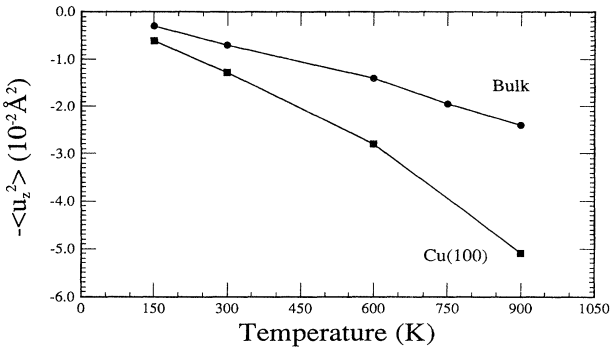

FIG. 8. One-dimensional (vertical) mean-square vibrational amplitudes of atoms on Cu(100) and in the bulk of Cu as functions of temperature.

From the table, at 300 K, for Ag(100) the vertical mean-square vibrational amplitude of the first-layer atoms is larger than that for the bulk atoms by a factor of 1.91, while for Cu(100) the enhancement factor is 1.83. For the second-layer atoms the increment factor is 1.3 for Cu and 1.4 for Ag, as compared to the bulk. As the temperature increases the departure of the surface vibrational amplitude from the bulk value becomes even larger. This is illustrated very effectively in Fig. 8, which also shows an appreciable change in the slope of the curves at about 600 K. It is interesting that a change of slope is registered in both the bulk and the surface curve in Fig. 8. The effect, however, is much stronger for the surface one. There appears then a further enhancement in anharmonic surface vibrational amplitudes at about 600 K. Such an onset has been found experimentally in the thermal attenuation of the diffracted He-atom or x-ray or low-energy-electron beam from Cu(100),[17] Cu(110),[15,16] Ni(110),[13] Ni(100),[14] and Al(110) (Ref. 42) and attributed to anharmonic effects or to thermal disorder or surface roughening. For Cu(100) our simulations indicate no evidence of disorder until 900 K and point to enhanced surface anharmonic vibrations as the reason for the large attenuation in the intensity of the diffraction beam.

V. CONCLUSION

From the comparison of our surface-parameter free molecular-dynamics simulations with the experimental data and first-principles calculation, on the Ag(100) and Cu(100) surfaces, it is concluded that the EAM potential can provide a reliable calculation of the interlayer relaxations and the surface phonon frequencies. The interesting features that we reproduce include a first-layer longitudinal mode at $\bar{M}$ and a second-layer shear vertical

mode at $\bar{X}$, which were not reported in earlier lattice-dynamics studies but revealed in recent first-principles calculations and EELS scattering cross-section calculations which include multiple-scattering events. We also find that a simple force-constant model can reproduce the main features of the phonon modes, but only when surface force constants are changed from the values in the bulk.

As shown in our studies of Cu(100) at three different temperatures, a molecular-dynamics study, as compared to lattice-dynamics studies, has the advantage of being able to explore the temperature effects on surface structural and vibrational properties such as relaxation, phonon frequency and linewidth, and mean-square vibrational amplitude of atoms. We have demonstrated here the effects of enhanced anharmonicity in the interaction potential for surface atoms, through the considerable broadening and redshift of the surface phonon modes and the large increase of the mean-square vibrational amplitude of surface atoms, as compared to those in the bulk, with increasing temperature.

ACKNOWLEDGMENTS

We thank Professor J. E. Black, Professor K. P. Bohnen, Professor S. Y. Tong, and Dr. C. Z. Wang for helpful discussions. The work of T. S. R. and L. Y. was partially funded by the National Science Foundation under Grant No. DMR900015P. MSD is supported in part by the Division of Materials Science, Office of Basic Energy Sciences, U.S. Department of Energy. Supercomputer time has been provided by the Pittsburgh Supercomputing Center.

[1]S. Lehwald, J. Szeftel, H. Ibach, T. S. Rahman, and D. L. Mills, Phys. Rev. Lett. **50**, 518 (1983).
[2]M. Wuttig, R. Franchy, and H. Ibach, Z. Phys. B **65**, 71 (1986).
[3]P. Moretto, M. Rocca, U. Valbusa, and J. E. Black, Phys. Rev. B **41**, 12 905 (1990).
[4]Y. Chen. S. Y. Tong, J.-S. Kim, L. L. Kesmodel, T. Rodach, K. P. Bohnen, and K. M. Ho, Phys. Rev. B **44**, 11 394 (1991).
[5]Y. Chen, S. Y. Tong, M. Rocca, P. Moretto, U. Valbuas, K. P. Bohnen, and K. M. Ho, Surf. Sci. **250**, L389 (1991).
[6]V. Bortolani, G. Santoro, U. Harten, and J. P. Toennies, Surf. Sci. **148**, 84 (1984).
[7]M. H. Mohamed, L. L. Kesmodel, B. M. Hall, and D. L. Mills, Phys. Rev. B **37**, 2763 (1988).
[8]J. S. Nelson, M. S. Daw, and E. C. Sowa, Phys. Rev. B **40**, 1465 (1989).
[9]K. Kern, R. David, R. L. Palmer, G. Comsa, and T. S. Rahman, Phys. Rev. B **33**, 4334 (1986).
[10]S. Lehwald, F. Wolf, H. Ibach, B. M. Hall, and D. L. Mills, Surf. Sci. **192**, 131 (1987).
[11]P. Zeppenfeld, K. Kern, R. David, K. Kuhnke, and G. Comsa, Phys. Rev. B **38**, 12 329 (1988).
[12]L. Yang and T. S. Rahman, Surf. Sci. **215**, 147 (1989).
[13]Y. Cao and E. H. Conrad, Phys. Rev. Lett. **64**, 447 (1990).
[14]Y. Cao and E. Conrad, Phys. Rev. Lett. **65**, 2808 (1990).
[15]P. Zeppenfeld, K. Kern, R. David, and G. Comsa, Phys. Rev. Lett. **62**, 63 (1989).
[16]R. Schneider, H. Dürr, Th. Fauster and V. Dose, Phys. Rev. B **42**, 1638 (1990).
[17]G. Armand, D. Gorse, J. Lapujoulade, and J. R. Manson, Europhys. Lett. **3**, 1113 (1987).
[18]A. P. Baddorf and E. W. Plummer, J. Electron. Spectrosc. Relat. Phenom. **54/55**, 541 (1990).
[19]J. S. Nelson, E. C. Sowa, and M. S. Daw, Phys. Rev. Lett. **61**, 1977 (1988).
[20]M. S. Daw and M. I. Baskes, Phys. Rev. B **29**, 6443 (1984).
[21]M. P. Allen and D. J. Tildesley, *Computer Simulation of Liquids* (Clarendon, Oxford, 1987).
[22]J. P. Hansen and M. L. Klein, Phys. Rev. B **13**, 878 (1976).
[23]M. Marchese, G. Jacucci, and M. L. Klein, Surf. Sci. **145**, 364 (1984).
[24]C. Z. Wang, A. Fasolino, and E. Tosatti, Phys. Rev. B **37**, 2116 (1988); F. Ancilotto, W. Andreoni, A. Selloni, R. Car, and M. Parrinello, Phys. Rev. Lett. **65**, 3148 (1990).
[25]S. M. Foiles, M. I. Baskes, and M. S. Daw, Phys. Rev. B **33**, 7983 (1986).
[26]W. Kohn and L. J. Sham, Phys. Rev. **140**, A1133 (1965).
[27]E. Clementi and C. Roetti, At. Data Nucl. Data Tables **14**, 177 (1974); A. De. McLean and R. S. McLean, *ibid.* **26**, 197 (1981).
[28]S. M. Foiles and M. S. Daw, Phys. Rev. B **38**, 12 643 (1988).
[29]M. Rocca, S. Lehwald, H. Ibach, and T. S. Rahman, Surf. Sci. **171**, 632 (1986).
[30]J. E. Black, D. A. Campbell, and R. F. Wallis, Surf. Sci. **115**, 161 (1982).
[31]*Metals: Phonon States and Electron States and Fermi Surfaces,* edited by K.-H. Hallwege and J. L. Olsen, Landolt-Börnstein, New Series Vol. 13 (Springer, New York, 1981).
[32]M. Wuttig, R. Franchy, and H. Ibach, Solid State Commun. **57**, 445 (1986).
[33]J. Ellis, E. M. McCash, and W. Allison, J. Electron. Spectrosc. Relat. Phenom. **54/55**, 325 (1990).
[34]J. L. Erskine, E. J. Jeong, J. Yater, Y. Chen, and S. Y. Tong, J. Vac. Sci. Technol. A **8**, 2649 (1990).
[35]H. L. Davis and J. R. Noonan, J. Vac. Sci. Technol. **20**, 842 (1982).
[36]Q. T. Jiang, P. Fenter, and T. Gustafsson, Phys. Rev. B **44**, 5773 (1991).
[37]K. A. Gschneidner, Jr., in *Solid State Physics,* edited by F. Seitz and D. Turnbull (Academic, New York, 1964), Vol. 16, p. 275.
[38]J. M. Moraboit, R. F. Steiger, and G. A. Somarjai, Phys. Rev. **179**, 638 (1969).
[39]E. R. Jones, J. T. McKinney, and M. B. Webb, Phys. Rev. **151**, 476 (1966).
[40]A. A. Maradudin and J. Melngailis, Phys. Rev **133**, A1188 (1964); B. C. Clark, R. Herman, and R. F. Wallis, Phys. Rev. **139**, A860 (1965).
[41]S. K. S. Ma, F. W. deWette, and G. P. Aldredge, Surf. Sci. **78**, 598 (1978).
[42]P. von Blanckenhagen, W. Schommers, and V. Voegele, J. Vac. Sci. Technol. A **5**, 649 (1987).